Mixed-Methodology-Based System-Level Simulation of Biochemical Assays in Integrated Microfluidic Systems

Y. Wang, A. S. Bedekar, S. Krishnamoorthy, S. S. Siddhaye, and S. Sundaram

CFD Research Corporation, Huntsville, AL, U.S.A., yxw@cfdrc.com

ABSTRACT

This paper presents a mixed-methodology-based modeling and simulation approach for system-level design of biochemical assays in microfluidic chips. The chip is broken down into a system of connected components (e.g., channels, junctions, and reactors) with relatively simple geometries and specific functions. Models are developed using analytical and numerical approaches (mixed methodology) to accurately capture the multi-physics behavior of individual components. These models have been integrated into a computational framework that enables rapid system-level simulation. Simulation results are validated against experimental data and numerical models. Our simulations achieve significant computational speedup (> 1,000-fold) without appreciably compromising accuracy (< 10% error relative to numerical analysis).

Keywords: microfluidic, assay, system-level simulation

1 INTRODUCTION

Microfluidic systems hold great promise for a wide spectrum of applications in biology, medicine, and chemistry. The tremendous advantages these miniaturized lab-on-a-chip systems offer over conventional approaches include substantial savings in samples, enhanced throughput, and automation. Multiphysics phenomena and the continuously growing integration level of microfluidic chips increase the complexity and difficulty of chip design. Although high fidelity numerical simulations enable accurate spatio-temporal analysis, the simulations can be prohibitively computationally expensive for design of integrated microfluidic systems, leading to long turnaround times. Previous system-level modeling efforts [1, 2] use over-simplified compact models that provide inadequate detail or require either laborious numerical analysis or experiments from users to extract process-related parameters.

To address this issue, this paper presents an accurate and efficient system-level modeling and simulation methodology for microfluidic bioassay design. We disassemble the chip into a connected network of simple components. Models for individual components are developed to accurately capture transport phenomena in the components (e.g., diffusion-based mixing, sample merging and splitting, and reactions). Specifically, volumetric reactors are formulated using the Method of Lines (MOL), and surface biochemical reactors are formulated using a two-compartment approach; both of which rely on the numerical solution of Ordinary Differential Equations (ODEs), while other components are analytically described. Proper parameters and algorithms are embedded in the component models to enable communication of transport information between adjacent components and integration of components into a system-level model. The model can be iteratively simulated at a fast speed to capture the effect on chip performance of a change in candidate designs.

2 SYSTEM DECOMPOSITION

Our approach is illustrated using an integrated enzyme kinetics analysis device (Figure 1a) studied by Schilling *et. al* [3]. It consists of sample and waste reservoirs, T-junctions and lysis and reaction channels. The T-junctions are further classified as merging or splitting junctions, depending on the main and branch flow directions. *E. coli* cells and lysis agent flow side by side into the long lysis channel (L3) to release the intracellular contents. The small intracellular molecules, such as enzyme β-galactosidase (β-gal), diffuse faster to the right half of the channel. At the splitting junction (S1), the flow stream is split and a fraction of the β-gal is extracted and transported via merging junction M2 to the reaction channel (VR1), where it reacts with the fluorogenic substrate β-D-galactopyranoside (RBG) and undergoes a Michaelis-Menten type enzyme reaction. The widthwise concentration profiles of the fluorescent reaction product (Resorufin) at different streamwise locations are used to extract the kinetic constants for the enzyme reaction.

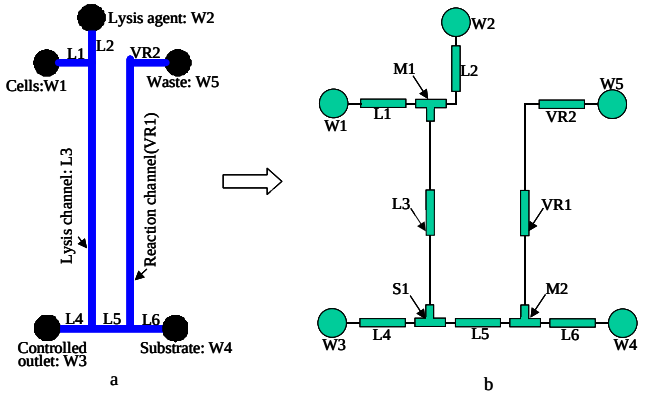

Figure 1. (a) A microfluidic device for cell lysis, extraction, reaction, and detection of intracellular components. (b) Its system-level representation.

In our approach, the chip is represented as a set of interconnected microfluidic components that include mixing channels (L1-L6), volumetric reactors (VR1, VR2), splitting junctions (S1), merging junctions (M1, M2), and wells (W1-W5) shown in Figure 1b. Components are connected by edges, which are considered 'wires' of zero resistance and convey transport information (e.g., flow rate and analyte concentrations) among adjacent components.

3 MODEL FORMULATION

Most microfluidic devices use either pressure-driven or electrokinetic flows to transport various analytes, buffers, and reagents. The compact model describing the fluid flow is derived using an integral form of the continuity and momentum equations, while that of the electric current is cast from the current conservation equation. The coupling between the mass and momentum conservation equations is achieved using an implicit pressure-based scheme. Modeling details are discussed elsewhere [4].

For sample transport, we consider two extensively used assays: volumetric and surface reactions. In the former, two streams carrying different analytes merge into another channel where they inter-diffuse and react in the entire channel. In surface reactions, free analytes flow through the channel and react with receptors immobilized on the bottom surface. Eq. (1) shows the generalized convection-diffusion equation governing the analyte concentrations $c(x, y, z, t)$ in axially fully developed flow for both volumetric and surface reactions.

$$\frac{\partial c_i}{\partial t} + u_i \frac{\partial c_i}{\partial x} - D_i \left(\frac{\partial^2 c_i}{\partial x^2} + \frac{\partial^2 c_i}{\partial y^2} + \frac{\partial^2 c_i}{\partial z^2} \right) - R_i = 0 \qquad (1)$$

where x, y, and z are the channel's axial, widthwise, and depthwise coordinates and aligned parallel to the flow, and perpendicular to the sidewalls, and bottom and top surfaces, and t denotes the time. The subscript i represents the quantities associated with the i^{th} free analyte in the stream. The flow field is represented by velocity u, while D is the diffusivity of the analyte. R is the volumetric reactive source term and depends on the reaction mechanism.

3.1 Volumetric Reactors

Since R_i in Eq. (1), in general, is nonlinear and does not allow for an analytical solution, a numerical technique, i.e., the Method of Lines (MOL) [5], is employed to achieve a fast and accurate solution. Specifically, assuming a large aspect ratio ($\beta = w/h >> 1$) and a large length-to-width ratio ($L/w >> 1$) of the channel, we can neglect the axial and depthwise diffusion of the analyte and approximate u by U in Eq. (1) [3][6], where L, w, and h are the channel length, width, and depth, and U is the cross-sectional average velocity of the analyte. The widthwise (y) diffusion term is discretized using the central differencing algorithm, resulting in a system of ODEs with independent variable x,

$$U_i \, \partial c_i^j / \partial x = D_i \left(c_i^{j-1} - 2c_i^j + c_i^{j+1} \right) \Big/ \left(\Delta y \right)^2 + R_i^j \qquad (2)$$

where Δy is the grid size; index j ($0 \le j \le J$) represents the quantities at the jth grid, and J is the total grid number in y. The MOL reduces the partial differential equation to a set of first order ODEs in x that can be easily solved using software packages developed specifically for numerical integration of large ODE systems.

We describe the reactive source term R_i for a Michaelis-Menten enzyme reaction, the mechanism for which can be written as $E + S \underset{k_{-1}}{\overset{k_1}{\rightleftarrows}} ES \xrightarrow{k_p} P + E$, where E, S, ES, and P represent the enzyme, substrate, enzyme-substrate complex, and product respectively [3]. k_1 and k_{-1} are the forward and backward rate constants of converting the enzyme and substrate to the enzyme-substrate complex, while k_p is the rate constant of converting enzyme-substrate complex to the product. Schilling *et. al* [3] show that for microfluidic assays that involve non-uniform analyte concentrations, the reactive source terms can be written as $R_s = -R_p = -k_p \, c_E \, c_S / (K_m + c_s)$ and $R_E = 0$ where K_m is the Michaelis constant.

3.2 Surface Reactors

For surface reactors, the principle of mass balance is applied to relate the *transient* cross-sectional average concentrations (rather than the *spatial* distribution) of analytes at component interfaces. In the text below, the average concentration of the free analyte is still denoted by c_i. The surface concentration of the immobilized receptors and bound analytes that do not enter the flow stream are notated by $\tilde{c}_i$ (unit: M·m).

The surface reaction induces a non-uniform analyte concentration along the channel depth z (independent of channel width y), which can be captured by a two-compartment model [7] shown in Figure 2. The reactor is divided into the surface compartment (close to the reactive surface) and the bulk compartment. In each compartment, the axially averaged (along x) analyte concentration is spatially uniform but varies with time. Applying a mass balance to the free analyte in the surface compartment [7] and the entire reactor, we can obtain

$$0 \approx -\tilde{q}_i + k_M \left(c_i^{(b)} - c_i^{(s)} \right) = -\tilde{q}_i + k_M \left(c_i^{(in)} - c_i^{(s)} \right) \qquad (3)$$

$$0 \approx -\tilde{q}_i A_{sur} + U_i A_c \left(c_i^{(in)} - c_i^{(out)} \right) \qquad (4)$$

where subscripts b, s, in, and out denote the quantities in the bulk and surface compartments and reactor inlet and outlet. In Eq. (3), the bulk analyte concentration is set equal to the fresh analyte concentration at the reactor inlet due to the thin concentration boundary layer. The reactive flux $\tilde{q}_i$ at the wall is assumed to be balanced by the mass transfer of the analyte to the surface, leading to a quasi-steady state of $c_i^{(s)}$ [7]. k_M is the mass transport coefficient that

characterizes the rate of analyte diffusion between the compartments [7]. In Eq. (4), A_{sur} is the surface area of the immobilized receptors; A_c is the channel's cross-sectional area; by the same token, a quasi-steady state assumption is also applied for the entire reactor.

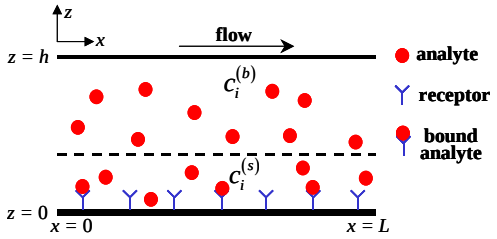

Figure 2. The two-compartment model in surface reaction.

In particular for a reversible analyte-receptor binding reaction $A + B \underset{k_d}{\overset{k_a}{\rightleftarrows}} AB$, the reactive analyte flux at the channel wall is: $-\tilde{q}_A = -k_a c_A^{(s)} \left(\tilde{c}_B^T - \tilde{c}_{AB}\right) + k_d \tilde{c}_{AB}$ where *A*, *B*, and *AB*, respectively, are the analyte, receptor site and bound analyte (or called analyte-receptor complex); k_a and k_d are the forward and backward rate constants. Thus, the average surface concentration of the analyte-receptor complex $\tilde{c}_{AB}$ is given by

$$d\tilde{c}_{AB}/dt = \tilde{q}_A = k_a c_A^{(s)} \left(\tilde{c}_B^T - \tilde{c}_{AB}\right) - k_d \tilde{c}_{AB} \qquad (5)$$

where $\tilde{c}_B^T$ is the surface concentration of total receptor binding sites and $\tilde{c}_B^T - \tilde{c}_{AB}$ is the available binding sites.

In addition to volumetric and surface reactors, other components, such as mixing channels and merging and splitting junctions and wells (Figure 1), have been modeled using analytical approaches (Fourier cosine series and algebraic equation) and discussed elsewhere [8]. To connect component models developed by disparate approaches, it is critical to determine common linking parameters conveyed through edges within the network. For the volumetric reaction, Fourier cosine series coefficients of the analyte concentration profile along the channel width $\left\{d_{i,n}^{(g)}\right\}^k$ [8] are selected, where the index *g* can be *in*, *out*, *l*, or *r*, respectively standing for the inlet, outlet, left, or right terminals of the component. The index *k* is the component number in the network. For the surface reaction, the average analyte concentration $\left\{c_i^{(g)}\right\}^k$ is employed. These parameters are propagated in the network as a signal flow. This means their values at the component's outlet are calculated based on the corresponding values at the inlet and contributions from the component itself. This information is then assigned as the input to the next component downstream (i.e., $\left\{d_n^{(in)}\right\}^{k+1} = \left\{d_n^{(out)}\right\}^k$ and $\left\{c_i^{(in)}\right\}^{k+1} = \left\{c_i^{(out)}\right\}^k$ [4]. In addition, to stitch the numerical volumetric reactor model (Eq. (2)) with analytical models characterized by Fourier coefficients (e.g., mixing channels and junctions [8]), a pre-reaction converter that translates d_n to discrete profiles c_i^j and a post-reaction converter that performs the reverse function are embedded in the reactor model and, respectively, given by

$$c_i^j = \sum_{n=0}^{\infty} d_{i,n} \cos\left(n\pi j/J\right) \text{ and } d_{i,n} = a_n \sum_{j=0}^{N} c_i^j \cos\left(n\pi j/J\right) \quad (6)$$

where $a_n = 1$ for $n = 0$ and $a_n = 2$ for $n \neq 0$. It should be emphasized that Eq. (6) allows us to minimize the use of the computationally expensive numerical ODE models to volumetric reactors only, rather than for the entire network. Thus, adequate simulation accuracy could be ensured without appreciably compromising the speed.

4 RESULTS AND DISCUSSION

Our system-level simulation results are shown in Figures 3–5. Figure 3 compares the results from the system-level simulation with detailed high fidelity simulations using CFD-ACE+^{TM} (ESI-CFD Inc., Huntsville, U.S.A) for widthwise concentration profiles of enzyme β-gal at different locations in the integrated chip in Figure 1. At the end of the lysis channel (station 1), an appreciable amount of enzyme β-gal is fractionated by stream splitting (S1) and transported to the next merging junction (M2), where it begins to react with the fluorogenic substrate (RBG). Therefore, at the immediate downstream (station 2) of the reaction channel, an abrupt concentration gradient is observed at the stream interface, which gradually smears out along the channel (station 3). Excellent agreement (relative error < 6.3 %) between system simulation and CFD-ACE+ results and tremendous speedup (10,000-fold) has been achieved. It should be pointed out that the concentration profile at position 2 is particularly important for determining rate constants of the reaction, which previously needed time-consuming numerical analysis [3].

Figure 4 shows the comparison between the system-level simulation results and experimental data on the widthwise concentration profile of the reaction product (Resorufin) extracted at 1 and 2.7 mm downstream of the reaction channel inlet. We use the same two-step simulation procedure formulated in [3] to take into account the different viscosities of sample and lysis agent streams. It can be seen that simulation and experimental data agree fairly well, although the predicted profiles shift slightly to the left. Since the enzyme reaction is fast relative to widthwise diffusion, Resorufin accumulates around the channel centerline leading to a concentration peak. With a constant input substrate concentration, this profile is uniquely determined by the enzyme concentration and rate constants, and can be used for both kinetics analysis and cell concentration measurements.

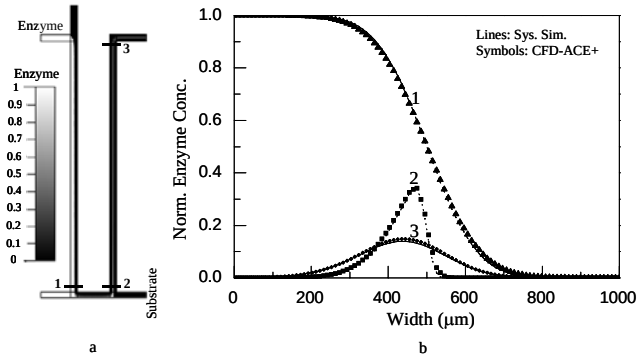

Figure 3. Comparison between system-level simulation and CFD-ACE+ results on the widthwise concentration profile of β-gal.

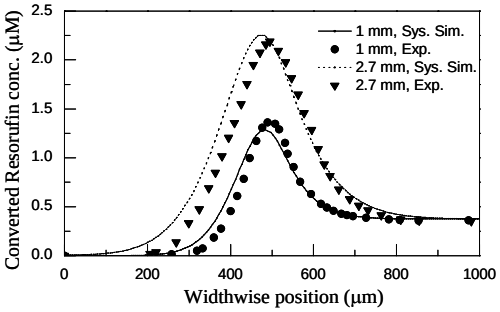

Figure 4. Comparison between system-level simulation results and experimental data on the concentration profile of Resorufin (enzyme reaction product).

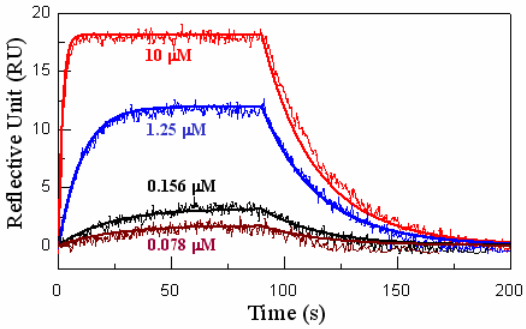

Figure 5. Comparison between system simulation and BIACORE data for binding of acetazolamide to surfaced immobilized anhydrase-II.

Figure 5 shows the comparison between transient system-level simulation (smooth curves) and BIACORE™ (BIACORE International, Uppsala, Sweden) data (fluctuating curves) on the Reflective Unit (RU) during the binding of acetazolamide (analyte) to surface-immobilized anhydrase-II (receptor). Here the change in RU from the Surface Plasmon Resonance measurement is linearly proportional to the surface concentration of the bound acetazolamide. The analyte supply was initiated at the beginning and then terminated at 90 s. We can see that the bound acetazolamide increases with time but at a decreasing rate, due to a reduction in available anhydrase-II binding sites as the reaction progresses and then levels off and reaches a steady state. After analyte supply was cut off, the bound analyte disassociates and restores to the initial state. In addition, as flow-in concentration of acetazolamide increases, reaction rate grows dramatically, leading to a fast approach to the equilibrium and a high equilibrium concentration. These response curves have been practically used in global analysis to extract the kinetic constants.

5 CONCLUSION

We have presented an efficient and accurate mixed-methodology-based system-level modeling and simulation approach for microfluidic bioassay design. Integrated chips are disassembled into a collection of simple components. Numerical ODE (Method of Lines and two-compartment approach) and analytical models are respectively obtained for reactors and other components that are linked to form a system-level representation of the entire chip. The system-level models are then applied to practical microfludic chips and validated against high-fidelity numerical analysis and experimental data. It shows that our models are able to accurately capture the overall effects of chip topologies, component geometries, and operational protocols on the chip performance. Compared with numerical methods, our simulation approach achieves a tremendous speedup (>1,000-fold), while still maintaining high accuracy (relative error less than 10 %). Therefore, it is well suited for iterative-simulation-based analysis and design of microfluidic assay chips. On incorporating optimization algorithms, the present effort can be readily extended to chip layout optimization and kinetics analysis.

ACKNOWLEDGEMENT

This research is sponsored by the National Aeronautics and Space Administration (Grant No. NNC04CA05C) and an internal R&D grant from CFD Research Corporation. The authors would like to thank Dr. Jerry W. Jenkins for providing and interpreting the BIACORE data and simulation parameters.

REFERENCES

[1] T. H. Zhang, K. Chakrabarty, R. B. Fair, IEEE Trans. Comput.-Aided Des. Integr. Circuits Syst., 23, 843, 2004.
[2] A. N. Chatterjee, N. R. Aluru, J. Microelectromech. Syst., 14, 31, 2005.
[3] E. A. Schilling, A. E. Kamholz, P. Yager, Anal. Chem. 74, 1798, 2002.
[4] A. S. Bedekar, Y. Wang *et. al*, IEEE Trans. Comput.-Aided Des. Integr. Circuits Syst., 25, 294, 2006.
[5] A. V. Wouwer, P. Saucez, W. E. Schieser, Ind. Eng. Chem. Res., 43, 3469, 2004
[6] M. A. Holden, S. Kumar *et. al*, Sens. Actuators B, 92, 199, 2003
[7] D. G. Myszka, X. He *et.al*, Biophys. J, 75, 583, 1998
[8] Y. Wang, Q. Lin, T. Mukherjee, Lab-on-a-Chip, 5, 877, 2005